Direct Dynamics Study of Hydrogen-Transfer Isomerization of 1-Pentyl and 1-Hexyl Radicals†

Jingjing Zheng and Donald G. Truhlar*

Department of Chemistry and Supercomputing Institute, University of Minnesota, Minneapolis, Minnesota 55455-0431

Received: April 10, 2009; Revised Manuscript Received: June 13, 2009

The rate constants of three intramolecular hydrogen-transfer isomerization reactions, namely, 1-4 isomerization of the 1-pentyl radical and 1-4 and 1-5 isomerizations of the 1-hexyl radical, are calculated using variational transition state theory with multidimensional tunneling, in particular by using canonical variational theory (CVT, which is the version of variational transition state theory in which the transition state dividing surface is optimized for a canonical ensemble) with small-curvature tunneling (SCT) for the transmission coefficient. The required potential energy surfaces were obtained implicitly by direct dynamics employing interpolated variational transition state theory with mapping (IVTST-M) and variational transition state theory with interpolated single-point energies (VTST-ISPE). Single-level direct dynamics calculations were performed for all of the reactions by IVTST-M using M06-2X/MG3S or M08-HX/cc-pVTZ+ potential energy surfaces or both. The stationary points of 1-4 isomerization of 1-pentyl and the stationary points for the forward reactions of 1-4 and 1-5 isomerizations of 1-hexyl were also optimized by BMC-CCSD, and for all three reactions we also performed dual-level direct dynamics calculations using VTST-ISPE in which MCG3-MPW single-point energies served as the higher level. The calculated MCG3-MPW//M06-2X/MG3S rate constants agree well with experimental values for 1-4 isomerization of the 1-pentyl radical at high temperature, and this validates the accuracy of this theoretical method for 1-4 isomerization. The MCG3-MPW//M06-2X/MG3S method was therefore used to make a reliable prediction for the rata constants of 1-4 isomerization of the 1-hexyl radical for which a direct experimental measurement is not available. The calculated CVT/SCT/M08-HX/cc-pVTZ+ rate constants agree well with experimental values for 1-5 isomerization of the 1-hexyl radical, and they show that the tunneling effect for these reactions was underestimated in previous work.

1. Introduction

Understanding the kinetics of normal alkyl radicals is important for combustion modeling of hydrocarbon fuels. Alkyl radicals are generated by the combustion of alkanes, and they can dissociate, isomerize, or react with oxygen.[1] The major isomerizations of the 1-hexyl radical are 1-4 and 1-5 intramolecular hydrogen transfers, which respectively occur through five- and six-member cyclic transition state structures. The 1−2 and 1−3 intramolecular hydrogen transfers are much less favorable because of large strain in the smaller rings of the transition state structures,[1,2] and they are not included in the present work.

It is difficult to measure reaction rates of alkyl radical isomerization directly, and therefore they have been derived by mechanistic analysis of complex processes such as thermal and photolytic decomposition processes. The first direct measurement of an alkyl radical isomerization reaction by Miyoshi et al.[3] was for 1-4 isomerization of the 1-pentyl radical. Experimental rate constants are also available for 1-5 hydrogen transfer isomerization of the 1-hexyl radical,[4−7] but there is no experimental measurement of the 1-4 hydrogen-transfer isomerization rate of this radical. Recently, Tsang et al.[7] reported 1-4 hydrogen-transfer isomerization rate constants for the 1-hexyl radical, but they were derived from experimental data on the 1-4 hydrogen-transfer isomerization of the 1-pentyl radical.[8−10] Experimental measurements of gas-phase unimolecular processes are always for finite pressures in the falloff regime; therefore, high-pressure limiting rate constants were derived from Rice−Ramsperger−Kassel−Marcus (RRKM)/master-equation analysis.

In interpreting some experimental work,[3,6,7] a simplified tunneling treatment, involving a zero-point inclusive[11] Eckart barrier[12] or parabolic barrier (Wigner approximation[12,13]), was used for the hydrogen-transfer processes; however, such treatments of tunneling are unreliable. Furthermore, the complexity of the mechanistic analysis used to infer rate constants contributes a large uncertainty to the experimental rate constants.[3,6,8−10] The scarceness and uncertainty of the experimental data provide an opportunity for theoretical modeling to clarify the rate constants.

Jitariu et al.[2] carried out dual-level direct dynamics calculations with canonical variational theory and the small-curvature tunneling approximation[14−17] (CVT/SCT) and the PUMP2-SAC/6-311G**///AM1 electronic structure method for decomposition and isomerization of the 1-pentyl radical, where /// denotes interpolated variational transition state theory with interpolated optimized corrections[18,19] (IVTST-IOC). Their calculated rate constants for 1-pentyl 1-4 hydrogen transfer isomerization are about a factor of 3 larger than experimental values[6] at 1000 K and at least a factor of 10 larger than experimental values[3,6,10] at 400 K, although a precise assessment is impossible at 400 K

† Part of the "Walter Thiel Festschrift".

* Corresponding author. E-mail: truhlar@umn.edu.

10.1021/jp903345x CCC: $40.75
Published on Web 07/17/2009

because the experimental rate constants[3,6,10] have large discrepancies at temperatures that low, and these values were derived from the data measured at higher temperatures. The aim of the present work is to calculate quantitatively accurate rate constants for 1-4 hydrogen-transfer isomerizations of 1-hexyl and 1-pentyl radicals and 1-5 isomerization of the 1-hexyl radical over a wide temperature range using variational transition state theory with multidimensional tunneling[14−17,20−25] (VTST/MT). Since many experimental data are available for 1-4 isomerization of the 1-pentyl radical, we performed calculations on this reaction first to validate the dual-level strategy used in the present work, and then we applied the strategy that performed best for 1-4 isomerization of the 1-pentyl radical to 1-4 isomerization of the 1-hexyl radical. We also calculated the 1-5 isomerization rate constants of 1-hexyl.

2. Theoretical Methods

2.1. Electronic Structure Calculations. The accuracy of the potential energy surface has a large effect on the accuracy of the calculated rate constants.[26] The M06-2X[27] and M08-HX[28] density functionals were used to optimize all of the stationary points on the potential energy surfaces for all three reactions as well as to perform dynamics calculations. Each stationary point was characterized as a minimum or a saddle point through normal-mode frequency analysis. Two multilevel methods, BMC-CCSD[29] and MCG3-MPW,[30] were used to calculate single-point energies at the stationary points, and BMC-CCSD was also used to optimize the stationary points of 1-4 isomerization of 1-pentyl and the stationary points for the forward reactions of 1-4 and 1-5 isomerizations of 1-hexyl.

Two basis sets, MG3S[31] and cc-pVTZ+,[32] were used in the density functional calculations. The MG3S basis is equivalent to the 6-311+G(2df,2p)[33] basis set for C and H. The cc-pVTZ+ basis is cc-pVTZ[34] for H and cc-pVTZ plus *s* and *p* diffuse functions from 6-31+G(d,p)[33] for C. The seven model chemistries[35] used here are M06-2X/cc-pVTZ+, M06-2X/MG3S, M08-HX/cc-pVTZ+, M08-HX/MG3S, BMC-CCSD, BMC-CCSD//M06-2X/MG3S, and MCG3-MPW//M06-2X/MG3S; single-point energy calculations of the barrier heights (with QCISD/MG3 geometries) have recently been assessed against the DBH24/08 database[36,37] and were found to be able to calculate barrier heights for diverse types of reactions with accuracies of 0.99 (M06-2X/cc-pVTZ+), 0.98 (M06-2X/MG3S), 0.90 (M08-HX/cc-pVTZ+), 1.14 (M08-HX/MG3S), 0.70 (BMC-CCSD), and 0.69 (MCG3S-MPW) kcal/mol, respectively. More specifically relevant to the present study is that the mean unsigned errors of M06-2X/cc-pVTZ+, M06-2X/MG3S, M08-HX/cc-pVTZ+, M08-HX/MG3S, BMC-CCSD, and MCG3-MPW (all //QCISD/MG3) are 1.30, 1.25, 0.65, 0.71, 0.63, and 0.44 kcal/mol, respectively, for hydrogen transfer, as assessed against the HTBH6 database.[37]

2.2. Dynamics. The high-pressure limit rate constants were calculated by CVT[14,20,21,25] with the SCT approximation.[15,16,25] A straightforward way to carry out a converged reaction-path calculation is to calculate electronic structure data (energies, gradients, and Hessians) for the whole range of the reaction path and to converge the calculation with respect to the density of points, but because of the large size of the pentyl and hexyl radicals, it is computationally burdensome to perform electronic structure calculations for every point on the reaction path using straight direct dynamics. Therefore, we used interpolated variational transition state theory by mapping[38] (IVTST-M) in all of the dynamics calculations; this method yields potential energy surface information along the full reaction path based on the data for a limited number of points along the portion of the reaction path near the saddle point. The details of the IVTST-M method can be found in the original paper;[38] here we only briefly summarize some aspects related to the present work.

For comparison we will also carry out some tunneling calculations using the Wigner approximation,[12,13] the parabolic tunneling approximation,[39] and the zero-curvature tunneling (ZCT) approximation.[11,25] In the Wigner or parabolic tunneling approximations, the transmission coefficient can be calculated analytically. In ZCT calculations, the kinetic energy coupling between the motion along the reaction coordinate and the motions of local vibrational modes is neglected; the tunneling path is the same as the isoinertial minimum-energy path, and the effective potential for tunneling is the ground-state vibrationally adiabatic potential.

For both CVT/SCT and CVT/ZCT, the final rate constant has the form $k^{CVT/MT} = \kappa^{CVT/MT} k^{CVT}$ where k^{CVT} is computed without tunneling or nonclassical reflection, $\kappa^{CVT/MT}$ is the multidimensional transmission coefficient, and MT is either SCT (final values) or ZCT (given only for comparison).

The IVTST-M method involves electronic structure calculations of only a subset of the needed information and generates the rest by a specialized spline-under-tension algorithm. The potential energy, the determinant of the moment of inertia tensor, the generalized normal-mode vibrational frequencies, and the small-curvature effective reduced mass at any point of the reaction path are obtained by interpolating the input data of the stationary points (reactant, product, and saddle point) geometries and Hessians, *H* nonstationary Hessians, and *G* geometries and nonzero gradients. We use the notation IVTST-M-*H*/*G* to denote using *G* geometries, energies, and gradients and *H* Hessians for nonstationary points in the interpolation, and we assume that there will be at least one gradient point beyond the farthest Hessian point in each direction to estimate the curvature components of the reaction path at the farthest out Hessian points by central differences of the gradient.

Curvilinear internal coordinates were used for generalized normal-mode analyses for stationary and nonstationary points.[17,40] A factor of 0.9721[27] is used to scale the M06-2X/MG3S frequencies. The M08-HX/cc-pVTZ+ frequencies are scaled by 0.9832, which was optimized in the present work by minimizing the root-mean-square errors to reproduce the zero-point vibrational energies in the ZPVE13/99 database.[41,42]

To generate the data used in interpolations, we first run a straight direct dynamics calculation using a small range of the reaction coordinate *s* from −0.50 Å to 0.50 Å (where distances are scaled to a reduced mass of 1 amu) by using the Page-McIver integrator[43] with a step size of 0.005 Å. We used M06-2X/MG3S or M08-HX/cc-pVTZ+ for these direct dynamics calculations. A Hessian matrix was calculated every 9 steps. Hence, 202 nonstationary points were calculated along the MEP, and Hessian matrices were calculated for 22 of them. The reaction paths over an extended range of the reaction coordinate from −4.50 Å to 4.50 Å with a step size of 0.005 Å were then obtained by interpolation using the IVTST-M-22/202 method.

To attempt to improve the barrier height and reaction energy calculated by density functional theory, we also run dual-level direct dynamics using variational transition state theory with interpolated single-point energies[19] (VTST-ISPE). In the VTST-ISPE method, the reaction path calculated at a lower level of theory, for example, M06-2X/MG3S, using the IVTST-M method is improved by using higher-level information consisting of single-point energies of the reactant, saddle point, and product. Here we used MCG3-MPW as the higher-level method.

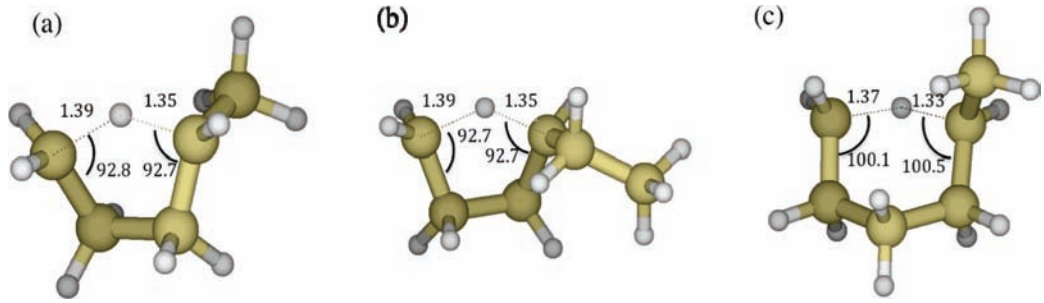

Figure 1. Optimized geometries of saddle points of the three hydrogen-transfer isomerizations: (a) 1-4 isomerization of 1-pentyl, (b) 1-4 isomerization of 1-hexyl, and (c) 1-5 isomerization of 1-hexyl.

TABLE 1: Calculated Forward and Reverse Zero-Point Exclusive Barrier Heights and Energies of Reaction for 1-4 Isomerization of 1-Pentyl and 1-Hexyl and and 1-5 Isomerization of 1-Hexyl (in kcal/mol)

rank[a]	method	$V_f^\dagger$	$V_r^\dagger$	ΔE
	1-4 Isomerization of 1-Pentyl			
1	MCG3-MPW//M06-2X/MG3S	24.11	27.07	−2.96
2	BMC-CCSD	24.46	27.17	−2.71
3	BMC-CCSD//M06-2X/MG3S	24.47	27.18	−2.71
4	M08-HX/cc-pVTZ+	25.31	28.69	−3.38
5	M08-HX/MG3S	25.17	28.58	−3.41
6	M06-2X/MG3S	25.53	28.81	−3.28
7	M06-2X/cc-pVTZ+	25.65	28.86	−3.21
	1-4 Isomerization of 1-Hexyl			
1	MCG3-MPW//M06-2X/MG3S	24.36	27.16	−2.80
2	BMC-CCSD	24.62		
3	BMC-CCSD//M06-2X/MG3S	24.63	27.16	−2.53
4	M08-HX/cc-pVTZ+	25.81	28.96	−3.15
5	M08-HX/MG3S	25.56	28.78	−3.22
6	M06-2X/MG3S	25.85	28.98	−3.13
7	M06-2X/cc-pVTZ+	25.95	29.05	−3.10
	1-5 Isomerization of 1-Hexyl			
1	MCG3-MPW//M06-2X/MG3S	17.29	20.24	−2.94
2	BMC−CCCSD	17.46		
3	BMC-CCSD//M06-2X/MG3S	17.47	20.16	−2.69
4	M08-HX/cc-pVTZ+	18.31	21.63	−3.32
5	M08-HX/MG3S	18.05	21.43	−3.38
6	M06-2X/MG3S	18.17	21.45	−3.28
7	M06-2X/cc-pVTZ+	18.32	21.57	−3.24

[a] The methods are ranked according to the assessment for hydrogen-transfer barrier height calculations in ref 37.

In such a case, we denote this VTST-ISPE calculation as MCG3-MPW//M06-2X/MG3S.

3. Results and Discussion

Figure 1 shows the key optimized geometric parameters for the saddle points of the 1-4 and 1-5 isomerizations of the 1-hexyl radical and the 1-4 isomerization of the 1-pentyl radical, as optimized by the M06-2X/MG3S method. The saddle-point structures of the 1-4 isomerizations of 1-pentyl and 1-hexyl are very similar five-membered rings. The distances of the transferring hydrogen to the donor or acceptor atoms are almost the same, with the hydrogen only slightly farther from 1-C than the acceptor. The geometries optimized by BMC-CCSD, M06-2X/cc-pVTZ+, M08-HX/MG3S, and M08-HX/cc-pVTZ+ are very similar to the M06-2X/MG3S ones in the figure. The Cartesian coordinates of the structures optimized with various methods are given in Supporting Information.

Table 1 lists the calculated zero-point exclusive barrier heights and energies of reaction for the 1-4 and 1-5 hydrogen transfer isomerizations of the 1-hexyl radical and the 1-4 isomerization of the 1-pentyl radical at various theoretical levels. Such barrier heights are sometimes called classical barrier heights. The BMC-CCSD//M06-2X/MG3S and MCG3-MPW//M06-2X/MG3S barrier heights and reaction energies agree with each other very well, and the BMC-CCSD (consistently optimized) barrier heights agree well with the BMC-CCSD//M06-2X/MG3S results, which validates the use of M06-2X/MG3S geometries in dual-level calculations for 1-pentyl and 1-hexyl. In general, the M06-2X and M08-HX calculations give higher barrier heights than BMC-CCSD, BMC-CCSD//M06-2X/MG3S, and MCG3-MPW//M06-2X/MG3S calculations. The calculated barrier heights are not sensitive to switching between the two basis sets MG3S and cc-pVTZ+. The maximum spread of all of the calculated barrier heights for any of the three forward barriers is 1.54 kcal/mol, and the maximum spread of all of the three reverse barriers is 1.89 kcal/mol.

The rate constants of the 1-4 isomerization of the 1-pentyl radical were calculated using the M06-2X/MG3S reaction path data generated with the IVTST-M-22/202 approach. This IVTST-M-22/202 calculation was also used as the lower level of a VTST-ISPE calculation, with the MCG3-MPW barrier height and reaction energy used as the higher level. The calculated CVT/SCT rate constants at the single level (IVTST-M) and dual level (VTST-ISPE) are plotted in Figure 2 along with the experimental data. Because Figure 2 extends over 14 decades, it is hard to see the important details. Therefore, we also present modified Arrhenius plots in which each rate constant k is divided by a temperature-dependent reference rate constant k_{ref}. The reference rate constant is given by the Arrhenius equation $k_{ref} = A \exp(-E_a/RT)$ using the activation energy E_a and prefactor A calculated by MCG3-MPW//M06-2X/MG3S (1-4 isomerization of 1-pentyl and 1-hexyl) and M08-HX/cc-pVTZ+ (1-5 isomerization of 1-hexyl) at 600 K. Note that E_a for each reaction is obtained from the local slope of a conventional Arrhenius plot (for example, Figure 2) at 600 K, and then A is obtained from k at 600 K. Thus k_{ref} is a local Arrhenius fit at 600 K. Figure 3 shows $\log(k/k_{ref})$ versus $1000/T$ for the 1-4 isomerization of the 1-pentyl radical. This figure shows the difference between experimental values and theoretical values more clearly.

The experimental data agree with each other quite well above 500 K, and the deviations of the calculated rates from the experimental ones are a factor of 1.7 or lower for temperatures above 500 K. The agreement between our calculated rate constants and experimental data at high temperature (above 500 K), where tunneling does not make a major contribution, indicates that the barrier height calculated by MCG3-MPW is accurate within about 0.5 kcal/mol. At temperatures below 500 K, the experimental data has large discrepancies. For example, the rate of Yamauchi et al.[6] is eight times smaller than the one of Miyoshi et al.[3] at 350 K. The possible reason for this large

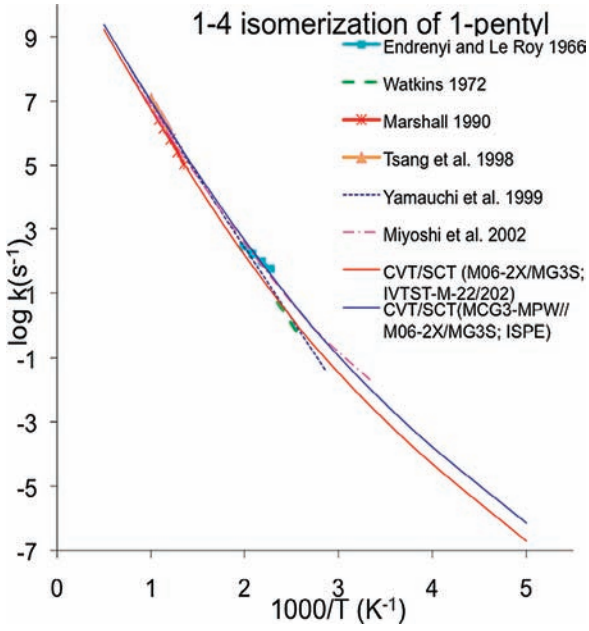

Figure 2. Arrhenius plots of calculated rate constants in this work and those obtained from the literature for 1-4 isomerization of the 1-pentyl reaction. The experimental data and their references shown are as follows: (1) Endrenyi and Le Roy (1966),[8] (2) Watkins (1972),[10] (3) Marshall (1990),[44] (4) Tsang et al. (1998),[45] (5) Yamauchi et al. (1999),[6] and (6) Miyoshi et al. (2002).[3]

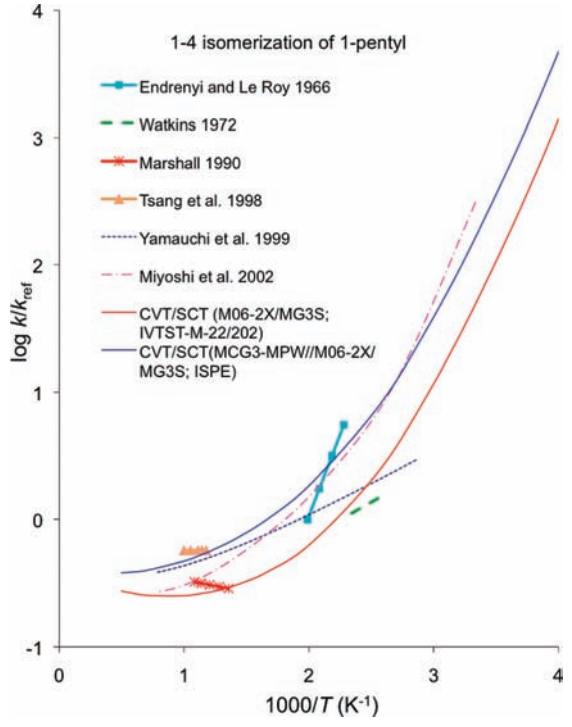

Figure 3. Plots of $\log(k/k_{ref})$ vs $1000/T$ for 1-4 isomerization of the 1-pentyl radical, where $k_{ref} = A \exp(-E_a/RT)$ using the activation energy E_a and the prefactor A calculated by MCG3-MPW//M06-2X/MG3S at 600 K.

discrepancy is because an Eckart potential was used to estimate tunneling when extracting rate expressions from the experimental data from higher temperature in the work of Miyoshi et al.,[3] whereas a Wigner approximation was used for this purpose in the work of Yamauchi et al.[6] Our calculated MCG3-MPW// M06-2X/MG3S dual-level CVT/SCT rate constants are in very good agreement with data of Miyoshi et al.[3] and are much larger than those of Yamauchi et al.[6] and Watkins[10] at temperatures

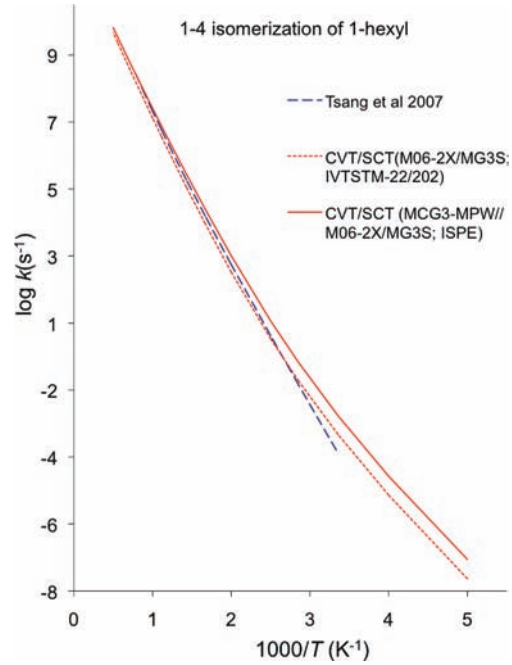

Figure 4. Arrhenius plots of calculated rate constants in this work and the data of Tsang et al.[7] for 1-4 isomerization of the 1-hexyl radical.

below 500 K. The data of Yamauchi et al.[6] and Miyoshi et al.[3] plotted in Figure 1 were calculated using their modified Arrhenius formulas, which are stated to apply to the temperature ranges of 350−1300 K and 300−1300 K, respectively. The data of Watkins[10] are for the temperature range 297−435 K.

The above comparison of the experimental and calculated rate constants for the 1-pentyl radical shows that MCG3-MPW// M06-2X/MG3S dual-level dynamics including the SCT approximation is quantitatively accurate for 1-4 isomerization reaction rate constants. Therefore, it is expected to make a reliable prediction for the 1-4 isomerization reaction of the 1-hexyl radical where a direct experimental measurement is absent. Figures 4 and 5 show an Arrhenius plot of the calculated rate constants and the data derived from 1-pentyl radical isomerization data by Tsang et al.[7] The MCG3-MPW//M06-2X/MG3S CVT/SCT rate constants agree with the high-temperature values based on the 1-pentyl radical data derived by Tsang et al. The calculated rates are much larger than the values of Tsang et al. below 500 K by factors ranging from 2 to 5. This indicates that Wigner correction used in the work of Tsang et al. underestimated the tunneling effect.

Direct dynamics calculations were also performed using the M06-2X/MG3S and MCG3-MPW//M06-2X/MG3S methods with IVTST-M-22/202 and VTST-ISPE dynamics for the 1-5 hydrogen-transfer isomerization of the 1-hexyl radical. The dual-level MCG3-MPW//M06-2X/MG3S rate constants are overestimated compared to the experimental data for the whole temperature range as shown in Figure 6 and as shown over a partial temperature range in Figure 7. This implies that the barrier heights calculated by M06-2X and MCG3-MPW are too low for this reaction although MCG3-MPW gives accurate barrier heights for 1-4 hydrogen-transfer isomerizations. Table 1 also shows that M08-HX/cc-pVTZ+ predicts a higher barrier height than the M06-2X/MG3S and MCG3-MPW methods. Therefore, direct dynamics calculations were performed using the M08-HX/cc-pVTZ+ method and IVTST-M-22/202 approach for 1-5 isomerization of the 1-hexyl radical. Figures 6 and 7 show that rate constants calculated using M08-HX/cc-

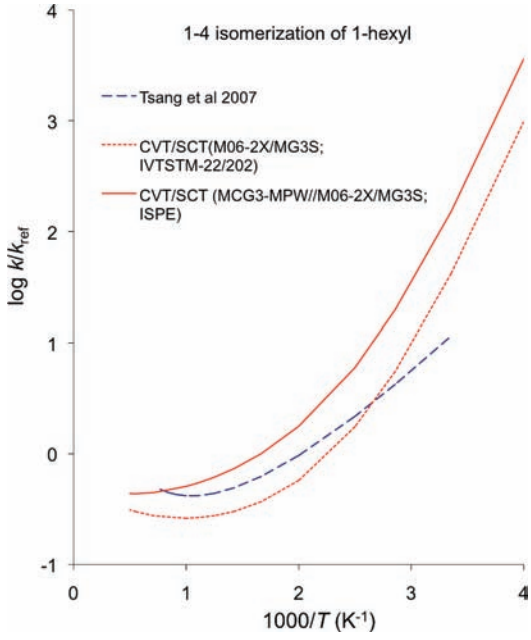

Figure 5. Plots of $\log(k/k_{ref})$ vs $1000/T$ for 1-4 isomerization of the 1-hexyl radical, where $k_{ref} = A \exp(-E_a/RT)$ using the activation energy E_a and the prefactor A calculated by MCG3-MPW//M06-2X/MG3S at 600 K.

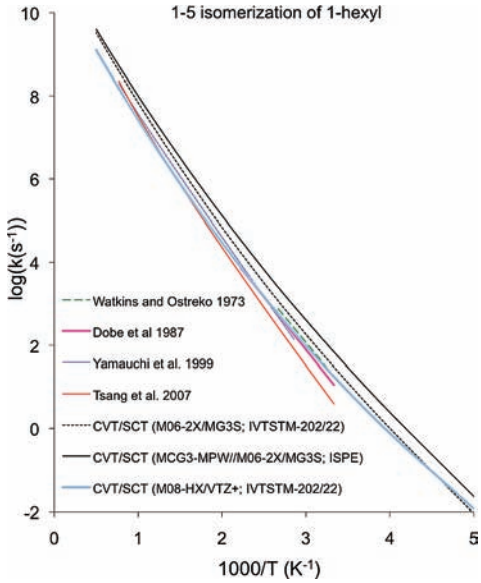

Figure 6. Arrhenius plots of calculated rate constants in this work and those obtained from the literature of 1-5 isomerization of 1-5 hexyl. The experimental data and their references shown are as follows: (1) Watkins and Ostreko (1973),[4] (2) Dobe et al. (1987),[5] (3) Yamauchi et al. (1999),[6] and (4) Tsang et al. (2007).[7]

pVTZ+ without further higher-level corrections agree with most experimental data very well. The rate constants of Tsang et al.[7] below 500 K are smaller than the others, but the discrepancy between the data of Tsang[7] and Yamauchi[6] is about a factor of about 2 for 350 K, which is smaller than the experimental errors (a factor of 3) of Yamauchi's data. In this sense, all experimental and calculated rate constants agree with each other within experimental errors. The dynamics calculations show that the M08-HX/cc-pVTZ+ barrier height is more accurate than those calculated at the BMC-CCSD//M06-2X/MG3S and MCG3-MPW//M06-2X/MG3S levels.

Parts a, b, and c of Figure 8 compare the transmission coefficients calculated by the Wigner, parabolic tunneling, ZCT,

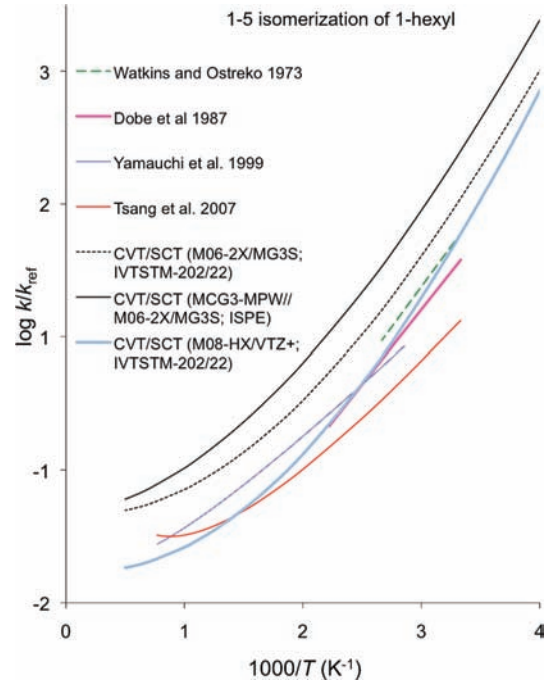

Figure 7. Plots of $\log(k/k_{ref})$ vs $1000/T$ for 1-5 isomerization of the 1-hexyl radical, where $k_{ref} = A \exp(-E_a/RT)$ using the activation energy E_a and the prefactor A calculated by M08-HX/cc-pVTZ+ at 600 K.

and SCT approximations, and part d compares the SCT transmission coefficients calculated for the three isomerization reactions studied in this work (the transmission coefficients are given in tabular form in Supporting Information). For 1-4 isomerization of the 1-pentyl radical, the Wigner transmission coefficients are in agreement with SCT calculations within 10% only for temperatures above 800 K; the SCT transmission coefficient is 1.56 at 800 K for 1-4 isomerization of the 1-pentyl radical. For 1-4 and 1-5 isomerizations of the 1-hexyl radical, the Wigner transmission coefficient agrees with the SCT one within 16% for temperatures at and above 1000 K. For 1-4 isomerization of 1-pentyl and 1-hexyl, the parabolic tunneling transmission coefficients agree with SCT calculations within 3% for temperatures above 500 K, which is even better than ZCT agreeing with SCT in this temperature range. For 1-5 isomerization of 1-hexyl, the parabolic tunneling calculations agree with ZCT calculations very well for the temperatures above 500 K, and both of them underestimate tunneling compared to the SCT calculations. At lower temperatures, the one-dimensional Wigner tunneling approximation significantly underestimates tunneling, and the parabolic tunneling approximation significantly overestimates tunneling. Figure 8d shows that the 1-hexyl radical has a very similar transmission coefficient to that of the 1-pentyl radical for 1-4 isomerization because they have very similar barrier heights calculated at the MCG3-MPW//M06-2X/MG3S level and their imaginary frequencies differ by only 6 cm^{-1} (see Supporting Information, Table S2). The 1-5 isomerization of the 1-hexyl radical has a much lower barrier than 1-4 isomerization; therefore, it has a smaller transmission coefficient than 1-4 isomerization. Figure 9 shows the calculated ground-state vibrationally adiabatic potentials versus the reaction coordinate s for the 1-4 isomerization of 1-pentyl and 1-hexyl and the 1-5 isomerization of 1-hexyl.

Since the Arrhenius plots are curved in Figures 2−7 for the three reactions studied here, the activation energy computed from the slope of the Arrhenius plot is temperature dependent.

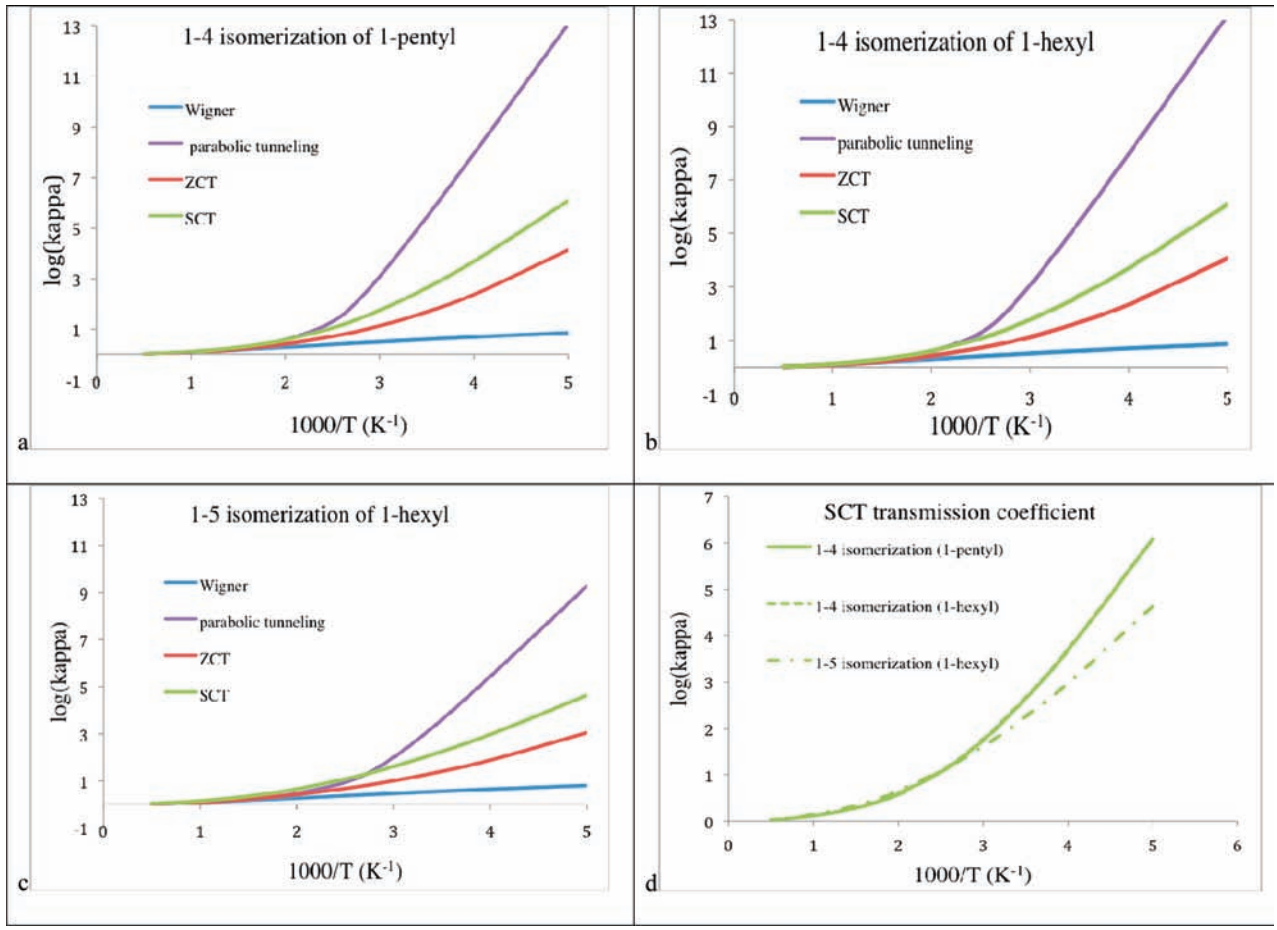

Figure 8. Calculated log κ vs 1000/T using the Wigner, ZCT, and SCT approximations. For 1-4 isomerizations of 1-pentyl and 1-hexyl, the MCG3-MPW//M06-2X/MG3S method was used. For 1-5 isomerization of 1-hexyl, the M08-HX/cc-pVTZ+ method was used.

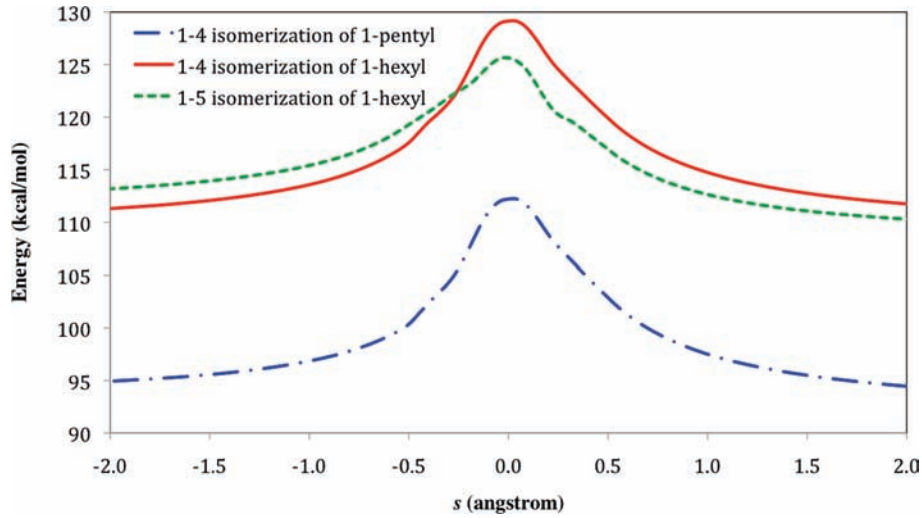

Figure 9. Calculated ground-state vibrationally adiabatic potentials (V_a^G) vs the reaction coordinate s for the 1-4 isomerization of 1-pentyl and 1-hexyl and the 1-5 isomerization of 1-hexyl.

Table 2 lists the activation energies for the three reactions at various temperatures using conventional transition state theory (TST, in which the transition state dividing surface is placed at the saddle point normal to the imaginary frequency normal mode), CVT, CVT/ZCT, and CVT/SCT approximations. The activation energy for a given temperature T was obtained by calculating the slope of the Arrhenius plot using rate constants at temperatures $T + 5$ K and $T - 5$ K. TST and CVT give very similar activation energies at each temperature for all three reactions. Tunneling significantly lowers the activation energies, especially at low temperatures. For example, the activation energies at 350 K are lowered by 8.4 and 6.0 kcal/mol for the 1-4 isomerization and the 1-5 isomerization, respectively.

The rate constants in Supporting Information show that the CVT rate constants without tunneling differ from the conventional TST ones by only about 10% for these reactions. By taking advantage of this, one could greatly simplify the calculations at temperatures where tunneling is not important.

TABLE 2: Activation Energies (kcal/mol) for the Three Isomerization Reactions at Various Temperatures (K)

	300	400	600	1000	1500
1-4 Isomerization (1-Pentyl) (MCG3-MPW//M06-2X/MG3S)					
TST	24.80	24.78	24.92	25.37	25.79
CVT	24.84	24.82	24.95	25.38	25.77
CVT/ZCT	19.58	21.60	23.25	24.48	25.19
CVT/SCT	16.41	19.53	22.53	24.22	25.04
1-4 Isomerization (1-Hexyl) (MCG3-MPW//M06-2X/MG3S)					
TST	24.97	24.96	25.10	25.54	25.96
CVT	24.99	24.99	25.13	25.56	25.96
CVT/ZCT	19.79	21.78	23.43	24.67	25.38
CVT/SCT	16.55	19.64	22.63	24.36	25.20
1-5 Isomerization (1-Hexyl) (M08-HX/cc-pVTZ+)					
TST	19.34	19.29	19.39	19.82	20.26
CVT	19.34	19.28	19.38	19.75	20.12
CVT/ZCT	15.55	16.61	17.71	18.77	19.42
CVT/SCT	13.34	14.87	16.74	18.31	19.14

However, faced with a new reaction, one does not know whether or not the variational effect (defined as the difference between the rate constant calculated by CVT and that calculated by TST) is important unless one carries out the variational calculation. Furthermore, if one is interested in high accuracy, one cannot neglect tunneling (in the present cases, tunneling increases the rates by 14−18% even at 1400 K, and at all temperatures below this it is quantitatively more important than the variational effect), and a reliable tunneling calculation requires enough information that it is relatively straightforward to produce the CVT rate constant as a byproduct.

4. Conclusions

The rate constants of the 1-4 hydrogen-transfer isomerizations of 1-pentyl and 1-hexyl radicals and the 1-5 isomerization of 1-hexyl radical were calculated using VTST/MT. The agreement between calculated rate constants and experimental values at high temperatures indicates high accuracy for the calculated barrier heights by the MCG3S-MPW//M06-2X/MG3S and M08-HX/cc-pVTZ+ methods. The MCG3S-MPW//M06-2X/MG3S method was used to make a reliable prediction for the rate constants of 1-4 isomerization of the 1-hexyl radical for which a direct experimental measurement is not available. The calculated CVT/SCT rate constants show that the tunneling effect for these reactions was underestimated by previous work at low temperatures.

Acknowledgment. The authors are grateful to Dr. Wing Tsang for suggesting this study and for helpful suggestions and discussion. This work was supported by the U.S. Department of Energy, Office of Basic Energy Sciences, under Grant No. DE-FG02-86ER13579.

Supporting Information Available: Cartesian coordinates of all of the reactants, products, and transition states optimized at various levels of theory; tabulated data for the plots in Figures 2−8; plots of the minimum energy path, the ground-state vibrationally adiabatic potential, and the generalized-normal mode vibrational frequencies along the reaction path. This material is available free of charge via the Internet at http://pubs.acs.org.

References and Notes

(1) Curran, H. J.; Gaffuri, P.; Pitz, W. J.; Westbrook, C. K. *Combust. Flame* **1998**, *114*, 149.
(2) Jitariu, L. C.; Jones, L. D.; Robertson, S. H.; Pilling, M. J.; Hillier, I. H. *J. Phys. Chem. A* **2003**, *107*, 8607.
(3) Miyoshi, A.; Widjaja, J.; Yamauchi, N.; Koshi, M.; Matsui, H. *Proc. Combust. Inst.* **2002**, *29*, 1285–1293.
(4) Watkins, K. W.; Ostreko, L. A. *J. Phys. Chem.* **1973**, *77*, 2938.
(5) Dobe, S.; Berces, T.; Reti, F.; Marta, F. *Int. J. Chem. Kinet.* **1987**, *19*, 895.
(6) Yamauchi, N.; Miyoshi, A.; Kosaka, K.; Koshi, M.; Matsui, H. *J. Phys. Chem. A* **1999**, *103*, 2723.
(7) Tsang, W.; Walker, J. A.; Manion, J. A. *Proc. Combust. Inst.* **2007**, *31*, 141–148.
(8) Endrenyi, L.; Le Roy, D. J. *J. Phys. Chem.* **1966**, *70*, 4081.
(9) Watkins, K. W. *J. Am. Chem. Soc.* **1971**, *93*, 6355.
(10) Watkins, K. W. *Can. J. Chem.* **1972**, *50*, 3738.
(11) Truhlar, D. G.; Kuppermann, A. *J. Am. Chem. Soc.* **1971**, *93*, 1840.
(12) Johnston, H. S. *Gas Phase Reaction Rate Theory*; The Ronald Press: New York, 1966.
(13) Wigner, E. P. *Z. Phys. Chem., Abt. B* **1932**, *19*, 203.
(14) Garrett, B. C.; Truhlar, D. G. *J. Chem. Phys.* **1979**, *70*, 1593.
(15) Lu, D. H.; Truong, T. N.; Melissas, V. S.; Lynch, G. C.; Liu, Y. P.; Garrett, B. C.; Steckler, R.; Isaacson, A. D.; Rai, S. N.; Hancock, G. C.; Lauderdale, J. G.; Joseph, T.; Truhlar, D. G. *Comput. Phys. Commun.* **1992**, *71*, 235.
(16) Liu, Y. P.; Lynch, G. C.; Truong, T. N.; Lu, D. H.; Truhlar, D. G.; Garrett, B. C. *J. Am. Chem. Soc.* **1993**, *115*, 2408.
(17) Jackels, C. F.; Gu, Z.; Truhlar, D. G. *J. Chem. Phys.* **1995**, *102*, 3188.
(18) Hu, W.-P.; Lu, Y.-P.; Truhlar, D. G. *J. Chem. Soc., Faraday Trans.* **1994**, *90*, 1715.
(19) Chuang, Y.-Y.; Corchado, J. C.; Truhlar, D. G. *J. Chem. Phys.* **1999**, *103*, 1140.
(20) Truhlar, D. G.; Garrett, B. C. *Acc. Chem. Res.* **1980**, *13*, 440.
(21) Truhlar, D. G.; Isaacson, A. D.; Skodje, R. T.; Garrett, B. C. *J. Phys. Chem.* **1982**, *86*, 2252.
(22) Truhlar, D. G.; Garrett, B. C. *Annu. Rev. Phys. Chem.* **1984**, *35*, 159.
(23) Truhlar, D. G.; Isaacson, A. D.; Garrett, B. C. In *Theory of Chemical Reaction Dynamics*; Baer, M., Ed.; CRC Press: Boca Raton, FL, 1985; Vol. 4; pp 65−137.
(24) Truhlar, D. G.; Garrett, B. C.; Klippenstein, S. J. *J. Phys. Chem.* **1996**, *100*, 12771.
(25) Fernandez-Ramos, A.; Ellingson, B. A.; Garrett, B. C.; Truhlar, D. G. In *Reviews in Computational Chemistry*; Cundari, T. R., Lipkowitz, K. B., Eds.; Wiley-VCH: Hoboken, NJ, 2007; Vol. 23; pp 125−232.
(26) Albu, T. V.; Espinosa-Garcia, J.; Truhlar, D. G. *Chem. Rev.* **2007**, *107*, 5101.
(27) Zhao, Y.; Truhlar, D. G. *Theor. Chem. Acc.* **2008**, *120*, 215.
(28) Zhao, Y.; Truhlar, D. G. *J. Chem. Theory Comput.* **2008**, *4*, 1849.
(29) Lynch, B. J.; Zhao, Y.; Truhlar, D. G. *J. Phys. Chem. A* **2005**, *109*, 1643.
(30) Zhao, Y.; Lynch, B. J.; Truhlar, D. G. *Phys. Chem. Chem. Phys.* **2005**, *7*, 43.
(31) Lynch, B. J.; Truhlar, D. G. *J. Phys. Chem. A* **2003**, *107*, 3898.
(32) Papajak, E.; Leverentz, H.; Zheng, J.; Donald, G. T. *J. Chem. Theory Comput.* **2009**, *5*, 1197.
(33) Clark, T.; Chandrasekhar, J.; Spitznagel, G. W.; Schleyer, P. V. *J. Comput. Chem.* **1983**, *4*, 294.
(34) Dunning, T. H., Jr. *J. Chem. Phys.* **1989**, *90*, 1007.
(35) Pople, J. A. *Rev. Mod. Phys.* **1999**, *71*, 1267.
(36) Zheng, J.; Zhao, Y.; Truhlar, D. G. *J. Chem. Theory Comput.* **2007**, *3*, 569.
(37) Zheng, J.; Zhao, Y.; Truhlar, D. G. *J. Chem. Theory Comput.* **2009**, *5*, 808.
(38) Corchado, J. C.; Coitino, E. L.; Chuang, Y. Y.; Fast, P. L.; Truhlar, D. G. *J. Phys. Chem. A* **1998**, *102*, 2424.
(39) Skodje, R. T.; Truhlar, D. G. *J. Phys. Chem.* **1981**, *85*, 624.
(40) Chuang, Y.-Y.; Truhlar, D. G. *J. Chem. Phys.* **1998**, *102*, 242.
(41) Fast, P. L.; Corchado, J.; Sanchez, M. L.; Truhlar, D. G. *J. Chem. Phys.* **1999**, *103*, 3139.
(42) Martin, J. M. L. *J. Chem. Phys.* **1992**, *97*, 5012.
(43) Page, M.; McIver, J. W., Jr. *J. Chem. Phys.* **1988**, *88*, 922.
(44) Marshall, R. M. *Int. J. Chem. Kinet.* **1990**, *22*, 935.
(45) Tsang, W.; Walker, J. A.; Manion, J. A. *Symp. (Int.) Combust., [Proc.]* **1998**, *27*, 135–142.

JP903345X